SPS/DI-MST/PEF/EEK 16th April, 1982.



SPS Improvement Report No. 193

# Commissioning of the low-beta insertions of the p-$\bar{p}$ collider

P.E. Faugeras, A. Faugier, A. Hilaire, A. Warman

E. d'Amico, L. Burnod, K.H. Kuhn, J.D. Pahud

Low-beta insertions have been installed in LSS4 and LSS5 and are used to focus the proton and antiproton beams at the crossing points in order to obtain a useful luminosity for the p-$\bar{p}$ collider. After a brief description of the insertions and of the associated hardware and controls, this report gives the main results of the commissioning experiments which allowed to reach betatron amplitudes of $\beta^*_H$ = 1.50m, $\beta^*_V$ = 0.75m at both crossing points simultaneously, which are lower than the nominal values of 2.0m x 1.0m. During a large fraction of the first p-$\bar{p}$ physics run of December 1981, both insertions were running at the same time, which gave a substantial increase of the luminosity of the collider, without any deterimental effect on the stored beams.

## 1. Description of the insertions

### 1.1 Insertion layout and matching

Both insertions have exactly the same layout in which a classical doublet on either side of the crossing point is used for focusing the beams, (1). In order to get the necessary focussing strength at 270 GeV, each lens of a doublet is made of a pair of identical quadrupoles, powered in series: the inner pairs use the lattice quadrupole 18 (pair upstream of the crossing point) and 19 (downstream pair), each being reinforced by another machine type quadrpuole, whose maximum gradient is 21 T/m for 2000 A. The outer quadrupole pairs are of the QWL type, formerly used in the SPS secondary beam lines, and capable of a maximum gradient of 17.5 T/m at 500 A. A free space of about 4 m in between the two pairs of each doublet is necessary for optical matching and is used for pulsed dipoles for closed orbit correction and for detectors ("Roman pots").

Matching of the betatron and dispersion functions from the crossing point to the regular lattice is done separately for the upstream and the downstream parts of the insertion. Apart from the doublet strengths, 5 machine quadrupoles on either side of the crossing point, i.e. no.13 to 17 upstream and 20 to 24 downstream, have to be adjusted independently. In addition a machine type quadrupole, QMC-217, has been installed in the missing magnet section in order to ease the matching of the downstream part of the insertion. The insertion region then extends from QD13 to QF24 included, which allows 15 independent parameters per insertion, whose values are determined by the matching routines of the AGS computer programme,(2).

This layout is quite flexible: various insertion configurations can be obtained by changing the doublet polarities and retuning the quadrupoles strengths, but without moving any elements. However, all commissioning experiments reported here were done with the FD-DF configuration: fig.1 shows the machine layout and the variations of the betatron and dispersion functions for the nominal beta values of $\beta_H^* = 2.0$m, $\beta_V^* = 1.0$m at the crossing point.

Owing to the large space of 28.9 m between quadrupoles 18 and 19, left free for the experiments, the betatron functions exhibit high maxima at the doublet quadrupoles. Although the vacuum chamber in these elements has been suitably shaped, the machine acceptance may be too small, especially in the horizontal plane, for injecting the beams at 26 GeV. To overcome this difficulty one can detune the insertions by progressively increasing the beta values at the crossing point, while keeping the aspect ratio $\beta_H^* / \beta_V^*$ constant and equal to 2, thus lowering the maxima of the betatron functions. For the FD-DF insertion of fig.1, the tuning range extends from $\beta_H^* = 1.5$m, $\beta_V^* = 0.75$ ($\hat{\beta}_H = 1706$m, $\hat{\beta}_V = 356$m) to $\beta_H^* = 7.0$m, $\beta_V^* = 3.5$m ($\hat{\beta}_H = 420$m, $\hat{\beta}_V = 86$.m), and fig. 2 shows the resulting continuous variations of the quadrupole strengths. One will then inject and accelerate the beams with the insertions on but detuned to these highest $\beta^*$s and "squeeze" the $\beta^*$s at high energy, just before storage, when the beam emittances are smaller. In this way one avoids the difficult transition from an unperturbed machine to the insertion configuration.

## 1.2 Hardware and controls

As already mentioned, 15 independent power supplies are necessary for feeding the insertion quadrupoles and matching each insertion. The power supplies connected to machine-type quadrupoles are capable of 2200 A maximum, whereas those associated to QWL pairs are limited to 500 A. The current regulation of each supply provides an absolute accuracy and a stability better than $\pm 10^{-4}$ of the full current.

Twelve by-pass switches per insertion have been installed underneath the machine quadrupoles 13 to 24 included, which allows to connect these quadrupoles either to the normal busbar feeding system when the insertions are not in service, or to their individual supply for low-beta operation. In addition, the polarity of each lens of the doublets and of each of the quadrupoles 16, 17, 20, 21 can be changed separately by invertor switches located in the corresponding power supply, in order to be able to set up different insertion configurations.

All the hardware associated with one insertion is controlled by a dedicated computer. Two sets of application programs have been written: at the lower level one can control individually each insertion quadrupole and its power supply through interactive displays as shown on fig.3. A global control is also provided which permits to set up completely a machine cycle with the insertion running, including the $\beta^*$ squeezing at high energy. Insertion matching is not possible on-line because this exceeds the capacity of the SPS control computers. It must be done beforehand with the AGS programme on the central CDC computer and the results, stored on a permanent file have to be transmitted first to the SPS service computer,(3). Using the proper magnetizing curves, the theoretical quadrupole strengths are then converted into current tables which are finally sent to the dedicated low-beta computers. Seen by the machine operator, this initialization program runs in a very similar way to the standard one without insertion (fig.4). As for the machine tunes, it is possible to adjust separately the strength of any insertion quadrupole at a given time of the cycle.

Finally, a mini-version of the AGS programme has been installed in the SPS consoles: it simply calculates and displays the betatronic functions without momentum errors, with the quadrupole strengths read either from library files or directly from the hardware. It can be used for instance to assess on-line the effect of a given change in a quadrupole strength on the machine tunes and on the pattern of the betatronic functions.

### 1.3 Closed orbit and chromaticity corrections

Because of the high values reached by the betatron functions at some of the insertion quadrupoles, any alignement error of one of these elements will strongly affect the closed orbit. This is of particular importance at injection when the beam emittances are big but also at high energy after the $\beta^*$ squeezing when $\hat{\beta}_H$ and $\hat{\beta}_V$ become rather large (see fig. 1). The hardware and software needed for closed orbit acqui-

sition and correction have therefore been modified accordingly, (4): 15 pulsed dipoles were installed in each insertion, some of them replacing the standard DC correcting dipoles normally used for low energy correction, the others being located at the centre of each doublet. The newly developed software can cope with a changing machine configuration by using the appropriate Twiss parameters at each corrector and/or position monitor location. The closed orbit can thus be fully corrected during the injection plateau, whereas the orbit distortions induced by errors in the insertions are minimized during the rest of the whole cycle.

Another consequence of the large maxima of the betatron functions is an increase of the linear machine chormaticities as well as the related higher order aberrations. This has necessitated the implementation of a new chromaticity correction cheme, which makes use of four interleaved sextupole families. The operation principles of this new system and its efficiency for the bare machine without insertions have already been reported, (5).

## 2. Test of a single insertion

### 2.1 Individual quadrupole testing

Before switching on a complete insertion, one started by verifying the polarity of each of its quadrupoles - which was not a trivial task - and the tracking accuracy of the associated power supply. This was done with a 26 - 400 GeV cycle, which allowed to have quadrupole currents up to 1800 A. The machine quadrupoles used in the insertion were successively taken out of the normal busbars and connected to their own power supply which was loaded with the same current waveform as for the standard lattice quadrupoles. No noticeable tune shift with respect to the unperturbed quadrupole layout could be observed on the beam at any energy.

For testing the QWL pairs, one has replaced the lattice quadrupoles 18 and 19 by the pairs QWL 177 and QWL 195 respectively and tried to restore the usual pattern of betatronic functions. However, because of the difference in position, this change induces a focusing defect which had to be compensated by powering suitably the neighbouring quadrupoles. One thus achieved a pseudo-insertion which could work up to 270 GeV only. Here the observed tune shifts agreed well with AGS calculations. Beam storage under these conditions showed the good stability of the power supplies.

These experiments which are based upon tune differences have allowed to test the correct functioning of each insertion element but are not accurate enough to measure properly their individual magnetizing curves.

## 2.2 The constant insertion

The next step was to set up a single insertion giving $\beta_H^* = 7.0$m, $\beta_V^* = 3.5$ m at the crossing point all along the 26-270 GeV cycle, i.e. without $\beta^*$ squeezing. The machine tunes $Q_H = 26.73$, $Q_V = 27.71$ were split by one integer which was not essential here but will become necessary later for the $\beta^*$ reduction to maintain a betatron phase advance close to 90° per period in both planes in the regular part of the SPS lattice.

In order to get the beam injected and circulating at 26 GeV with this machine configuration, one had to lower $Q_H$ by about 0.15 whereas $Q_V$ was approximately right, which suggested that the gradient of the QWL quadrupoles was not as expected at 26 GeV. Indeed at the location of both QWL pairs, $\beta_H \simeq 400$ m and $\beta_V \simeq 20$m, and an error $\Delta k$ in their normalized strength would produce a tune shift

$$\Delta Q = \frac{1}{4\pi} \beta \cdot \Delta K \cdot \ell \qquad (1)$$

20 times larger for $Q_H$ than for $Q_V$. None of the other insertion quadrupoles could induce such a large effect which should have been seen by the previous individual tests. Simulation with the mini-AGS programme of the console showed that an error of about 2% in both QWL pairs gives $\Delta Q_H = .16$ $\Delta Q_V \simeq .02$. As a result this mismatch of the insertion produces a large "beating" of $\beta_H$ in the regular part of the machine : fig.5 shows that instead of equal maxima of $\beta_H$= 108m at each QF location outside the insertion region, $\beta_H$ reaches 200 m at locations 20, 24, 28... in each sextant and only about 60 m at the other locations 22, 26, 30..., whereas $\beta_V$ is hardly affected.

This assumption was confirmed experimentally by measuring the local betas at positions 1 - 10 and 1 - 28 by pulsing the small quadrupoles LQF - normally used for stop band correction - and by measuring the resulting tune shifts. One thus obtained :

position 1 - 10 $\quad \beta_H = 67 \pm 10$ m $\quad \beta_V \simeq 20$ m

position 1 - 28 $\quad \beta_H = 190 \pm 20$ m $\quad \beta_V \simeq 23$ m

which agrees fairly well with the simulation.

At high energy the local betas were measured by varying slightly the strength of one of the quadrupoles of the other insertion and no beating was observed at 270 GeV within the accuracy of the measurements. It was then concluded that the remanent field of the QWL quadrupoles was higher than anticipated, which was confirmed afterwards by further measurements in the labs, (6). Note that the insertion quadrupoles cannot be demagnetized in between two successive machine cycles.

After a suitable modification of the magnetizing curve of the QWL's it was no longer necessary to lower $Q_H$ for getting the beam circulating

and the insertion was found correctly matched at all energies.

## 2.3 The $\beta^*$ squeezing

For reducing the $\beta^*$ at high energy one must translate first the squeezing curves of fig.2 into proper current waveforms for the insertion quadrupoles, which is done in the initialization programme (see above) in the following way. Each intermediate insertion is characterized by the squeezing factor SQ defined by:

$$\frac{1}{SQ} = \sqrt{\frac{\left(\beta_H^* \cdot \beta_V^*\right)_{actual}}{\left(\beta_H^* \cdot \beta_V^*\right)_{initial}}} \qquad (2)$$

One then assigns somewhat arbitrarily a suitable variation of SQ with the time in the machine cycle, which allows to calculate the current tables to be sent to each power supply, using the squeezing curves of fig. 2 and the adequate magnetizing curves. As the betatron phase advances through the insertion depend very much on the actual $\beta^*$s, the normal lattice quadrupoles QF and QD must also be included in this process in order to maintain a constant working point during the $\beta^*$ squeezing.

For the time dependence of the squeezing factor SQ one has chosen a cubic shape, starting with a zero slope 0.18 sec after the beginning of the 270 GeV flat top and ending 1.2 sec later, again with a zero slope. In this way one avoids any transient in the power supplies and fig. 6 shows some of the resulting current waveforms.

No loss of beam was experienced during this $\beta^*$ reduction and after

it for the rest of the high energy flat top. It was only necessary to optimize the working point - the maximum correction on the lattice quadrupoles did not exceed $\Delta Q = .04$, as compared to the calculated values - and to adjust the chromaticity sextupoles in order to cope with the larger chromatic aberrations associated with the lower $\beta^*$s. Beam storage under these conditions showed again the excellent stability of the insertion power supplies and gave a beam lifetime comparable to what it was without insertion.

## 3. Running-in of two constant insertions

Although the $\beta^*$ squeezing process has been shown to work, it was preferred for the first $p-\bar{p}$ physics runs to start with the less ambitious configuration in which $\beta^*_H = 7m$ $\beta^*_V = 3.5$ m at both crossing points simultaneously, but kept constant all along the cycle. Commissioning of these "moderate" insertions gave the following results:

### 3.1 Insertion matching

One has checked first that there was no noticeable beating for $\beta_H$ outside the insertions at low energy by using as before the harmonic corrections LQF 1 - 10 and 1 - 28. This test cannot be performed at high energy as no pair of quadrupoles is suited for this measurement: the extraction quadrupoles - the only available elements - are badly phased in this respect.

Another way to assess the matching is to measure the local betas inside each insertion by varying slightly the strength of one of the insertion quadrupoles and observing the resulting tune-shifts. Instead of calculating the $\beta$'s with eq.(1), which gives an average over the quadrupole length, one has compared directly the measured tune shifts with those calculated with the mini AGS of the console and Table I gives some of the results.

Table I

| Insertion Quad | $\frac{\Delta k}{k}$ | 26 GeV | | 270 GeV | | calculated | |
|---|---|---|---|---|---|---|---|
| | | $\Delta Q_H$ | $\Delta Q_V$ | $\Delta Q_H$ | $\Delta Q_V$ | $\Delta Q_H$ | $\Delta Q_V$ |
| QW 4177 | -1% | -.035 | +.008 | -.028 | +.001 | -.029 | +.002 |
| Q 418 | +4% | -.030 | +.029 | -.032 | +.029 | -.028 | +.027 |
| Q 419 | +4% | -.035 | +.035 | -.032 | +.029 | -.031 | +.029 |
| QW 4195 | -1% | -.038 | +.007 | -.030 | -.001 | -.033 | +.001 |
| QW 5177 | -1% | -.035 | +.008 | -.025 | +.002 | -.029 | +.002 |
| Q 518 | +4% | -.030 | +.029 | -.029 | +.028 | -.028 | +.027 |
| Q 519 | +4% | -.034 | +.028 | | | -.031 | +.029 |
| QW 5195 | -1% | -.041 | +.003 | | | -.033 | +.001 |

In view of the accuracy of the Q-measurements, especially at 26 GeV, the agreement with the calculations is quite satisfactory. It is not possible to increase $\Delta k/k$ for improving the accuracy on the measured tune shifts as one is limited by third integer and coupling resonances.

### 3.2 Closed orbit correction

Several methods were tried for correcting the closed orbit at 26 GeV, using the new software which had to be developed to cope with the new monitors and correctors installed and with the irregularities induced in the machine lattice by the insertions, (6). The best results

were obtained in the following way. The beam is first centered with the insertions on and with zero current in the correcting dipoles by adjusting the main bending field. Then the beam position monitors 15 to 22 inclusive of both LSS4 and LSS5 are disconnected by software and the Twiss parameters corresponding to the machine configuration and working point are loaded. This allows to correct the orbit globally outside the insertion regions by the usual beam dump method. After having reconnected the pick-ups 15 to 22 of LSS4 and LSS5, one can now minimize the orbit excursions inside the insertion regions by special bump. Figure 7 shows the result of this procedure: outside the insertions, the peak-to-peak residual closed orbit deformation is of the order of 2mm and quite comparable to what it is without insertion. (In this figure, the crosses indicate position monitors which are disconnected).

At high energy a global correction is not possible as there are only a few pulsed dipoles in the insertion regions and in LSS3. One then minimizes the peak-to-peak amplitude of the orbit by the method of the best kick. Usually one or two kicks per plane are sufficient to bring the orbit amplitude within acceptable limits. Figure 8 shows that the peak-to-peak values are lower than for a machine without insertions, but without local kicks. Correction inside the insertions can now proceed, but is much more difficult than at 26 GeV, as it may perturb the previous minimization.

### 3.3 Chromatic measurements

The linear chromaticities were measured first at 26 GeV, 270 GeV and during the ramp. This allowed to have nearly zero chromaticity all along the cycle by adjusting accordingly the three coefficients a,b,c which control the variation of the linear corrections $\Delta\xi$ with the time of the cycle:

$$\Delta\xi = a + b\,\frac{B_{inj}}{B} + c\,\frac{1}{B}\cdot\frac{dB}{dt} \qquad (3)$$

One then looked at the variations of the machine tunes with the momentum deviation at 26 GeV and at 270 GeV. (Fig.9). During the injection flat bottom, $Q_V$ is almost flat whereas $Q_H$ varies quadratically with $\Delta p/p$: this residual curvature is more pronounced than for the bare machine because of the insertions (compare with Fig. 3 of Ref. 5) and both $Q_H$ and $Q_V$ variations agree fairly well with AGS predictions. At 270 GeV, $Q_V$ is still practically flat, but here $Q_H$ has a slight cubic dependence with the momentum deviation. This effect has already been observed for the machine without insertions (5) and is due to the decapolar component of the field of the main bending magnets coming from their saturation. Here again the experimental curves agree well with the theoretical predictions, which shows that the new sextupole correction scheme works as expected.

Finally, the constant term a of eq.(3) was raised by .1 in each plane, to ensure that $\xi_H$ and $\xi_V$ remain slightly positive during the whole machine cycle.

### 3.4 Beam storages

Storages of single bunches of protons only gave a proton lifetime in excess of 100 hours (1/e decay), which means that there is no degradation whatsoever of the single beam performances with this machine configuration, as compared to the bare machine without insertions.

Antiprotons were therefore injected and several $p-\bar{p}$ physics runs took place under these conditions. At the beginning of the coast, the antiproton lifetime was of the order of several hours, but increased rapidly over one hour to reach a steady value ranging from 25 to 40 hours, depending on the antiproton emittances. No direct measurement of the luminosity was available; however, the rate of trigger events, seen by the users, was increased by about a factor 10 with respect to runs without insertions for similar beam parameters,showing that the

luminosity is increased as expected (theoretical gain : 9.8).

## 4. Two squeezed insertions

Only one development session was devoted to the setting-up of two insertions simultaneously squeezed down to $\beta_H^* = 1.5$ m, $\beta_V^* = .75$ m at high energy. This was done with the same procedure as in para. 2.3, but here one was using an overall squeezing factor:

$$SQ = SQ_{LSS4} \cdot SQ_{LSS5} \qquad (4)$$

for determining the current waveforms of the insertion quadrupoles. Also at any time of the cycle the $\beta^*$s are kept the same for both crossing points, i.e. $SQ_{LSS4} = SQ_{LSS5}$.

### 4.1 Machine tuning and insertion matching

After adjustment of the working point and of the chromaticity sextupoles, no loss of beam was experienced during and after this double squeezing. Here also it was not possible to verify the absence of beating outside the insertions. However, the adjustments of the lattice quadrupoles needed for maintaining a constant working point throughout the machine cycle did not exceed $\Delta Q = .05$, which is a good indication of a correct matching. The tune shifts resulting from small demanded changes on the doublet lens strengths were measured after squeezing with the following results:

Table II

| Quadrupole Pair | $\frac{\Delta k}{k}$ | measured $\Delta Q_H$ | measured $\Delta Q_V$ | calculated $\Delta Q_H$ | calculated $\Delta Q_V$ |
|---|---|---|---|---|---|
| QW 4177 | -.2% | -.028 | +.004 | -.025 | +.002 |
| Q 418 | +1% | -.034 | +.028 | -.027 | +.029 |
| Q 419 | +1% | -.033 | +.031 | -.030 | +.032 |
| QW 4195 | -.2% | -.033 | +.008 | -.029 | +.002 |
| QW 5177 | -.2% | -.030 | +.008 | -.025 | +.002 |
| Q 518 | +1% | -.029 | +.027 | -.027 | +.029 |
| Q 519 | +1% | -.035 | +.031 | -.030 | +.032 |
| QW 5195 | -.2% | -.034 | +.007 | -.029 | +.002 |

Again the agreement is quite satisfactory, but a better accuracy on the tune shifts could be obtained during storage by measuring the betatron frequencies with the Schottky noise detectors (7).

### 4.2 Closed orbit and chromaticity corrections

With the same high energy corrections as for the constant insertions, the peak-to-peak amplitudes of the closed orbit become 32.5 mm horizontally and 16.2 mm vertically after the squeezing. The method

of the best kick has allowed to reduce them down to 15.5 mm horizontally and 9.4 mm vertically (fig. 10), again comparable to what is observed on the machine without insertions. Local corrections inside the insertion were not tried. It is worth mentioning that, with the synchrotron light monitors, (8), the beam was seen to be moving during the squeezing process, but this effect is much less pronounced than during the round-off which preceeds the 270 GeV flat top.

The same chromatic corrections as for the constant insertions were kept here during injection and acceleration. In particular the coefficients of eq.(3) were left untouched. In order to cope with the increased linear chromaticities due to the $\beta^*$ reductions, calculated trims were simply added at high energy (fig.11). Looking at the variations of the machine tunes with the momentum deviation revealed quite a comfortable momentum window (see fig. 12, in which $\Delta R$ (mm) $\simeq \Delta p/p$ (o/oo)), in fact larger than anticipated. While $Q_V$ behaves practically as expected, the $Q_H$ behaviour is in disagreement with AGS simulations, which predict a larger and negative curvature. Moreover, the decapolar component of the bending field should induce a cubic term with a sign opposite to what is observed (compare fig. 9 and 12). It is difficult to invoke an insertion mismatch and/or a sextupole mistuning to explain this discrepancy and the reason for it remains to be found. Also chromaticity measurements during beam storage should be done to confirm this fortunate improvement.

### 4.3 Beam storages

Only a few shots with antiprotons were tried with this machine configuration. The proton lifetime was still of the order of 100 hours and for relatively low antiproton intensity and emittances, the antiproton lifetime increased as before from a few hours at the beginning of the coast to a steady value around 30 hours. Figure 13 shows the evolution of the antiproton current during a coast which lasted 7 hours.

When increasing the antiproton bunch intensity, nominal luminosities

ranging from 1 to 5 x $10^{27}$ $cm^{-2}$ $s^{-1}$ were recorded. Unfortunately, at that time a high background in the p-$\bar{p}$ experiments was reported, which limited the benefit expected from the luminosity increase. The reason for the background could not be found. It may be due to the squeezed insertions: with this configuration the machine is very sensitive to any parameter change and needs to be carefully tuned. It may also come for more trivial reasons like large antiproton emittances and/or instability in one of the machine components : another p-$\bar{p}$ run performed without insertions at all, also led to high background, which suddenly disappeared on the subsequent shot.

## 5. Conclusion

Feasibility of operating the SPS collider with two low-beta insertions has clearly been demonstrated. In particular the configuration which gives $\beta_H^*$ = 7.0 m, $\beta_V^*$ = 3.5 m at both crossing points, without $\beta^*$ squeezing can be considered as operational and has already led to a luminosity increase of about 10, as expected. Squeezing the $\beta^*$ at high energy down to $\beta_H^*$ = 1.5 m, $\beta_V^*$ = .75 m at the two crossing points simultaneously has also been shown to work without any detrimental effects on the stored beam lifetimes. However, to fully benefit from this procedure and put it into operation, more measurements are needed to verify the correct insertion matching, to understand the behaviour or the horizontal chromaticity and to assess the dynamic machine acceptance. Also other insertion configurations must now be tried, as for instance the "high beta" in LSS4 which would give $\beta_H^*$ = $\beta_V^*$ = 100 m, for small angle scattering experiments. It may finally be interesting to test a fully antisymmetric configuration giving $\beta_H^*$ = $\beta_V^*$ = 1 m, at both crossings, in case the observed coupling between the two transverse planes cannot be corrected.

Acknowledgements

Design and installation of the hardware linked to the low-beta insertions have involved quite a number of people in the SPS Division, in particular in the AMR, APS, ABM and SEL groups. A few of the operation crews have also participated in some of the measurements. Thanks are due to them, with apologies for not being able to mention them all.

REFERENCES

1. P. FAUGERAS, A. FAUGIER, A. HILAIRE,
The low-beta insertions in the SPS and their chromaticity correction, Proceedings of the XIth Int.Conf. on High-Energy Accelerators, Geneva, 1980 (CERN/SPS/80-11(AC).

2. E. KEIL, Y. MARTI, B.W. MONTAGUE, A. SUDBOE,
AGS - The ISR computer program for synchrotron design, orbit analysis and insertion matching. CERN 75-13, 1975.

3. P. FAUGERAS, CERN/SPS/AC/Int.Note/80-4, July, 1980.
V. FRAMMERY, SPS/ACC-SW/VF/Computer Note 81-07, Feb. 1981.
A. FAUGIER, A. WARMAN, SPS/AOP/Note/81-5, April, 1981.

4. L. BURNOD, E. d'AMICO, J. MILES,
Software for closed orbit acquisition and correction in a variable configuration, CERN SPS/82-5 (ABM), March, 1982.

5. P. FAUGERAS, A. FAUGIER, A. HILAIRE, A. WARMAN,
The new chromaticity correction scheme of the SPS,
SPS Improvement Report No. 184.

6. W. NAGELE, private communication, Dec. 1981.

7. T. LINNECAR, W. SCANDALE,
Schottky scan measurements during 1981, SPS Improvement Report No. 192, February 1982.

8. R. BOSSART, et al,
Proton beam profile measurements with synchrotron light, Nuclear Int. and Meth., 184,349, 1981.

* * *

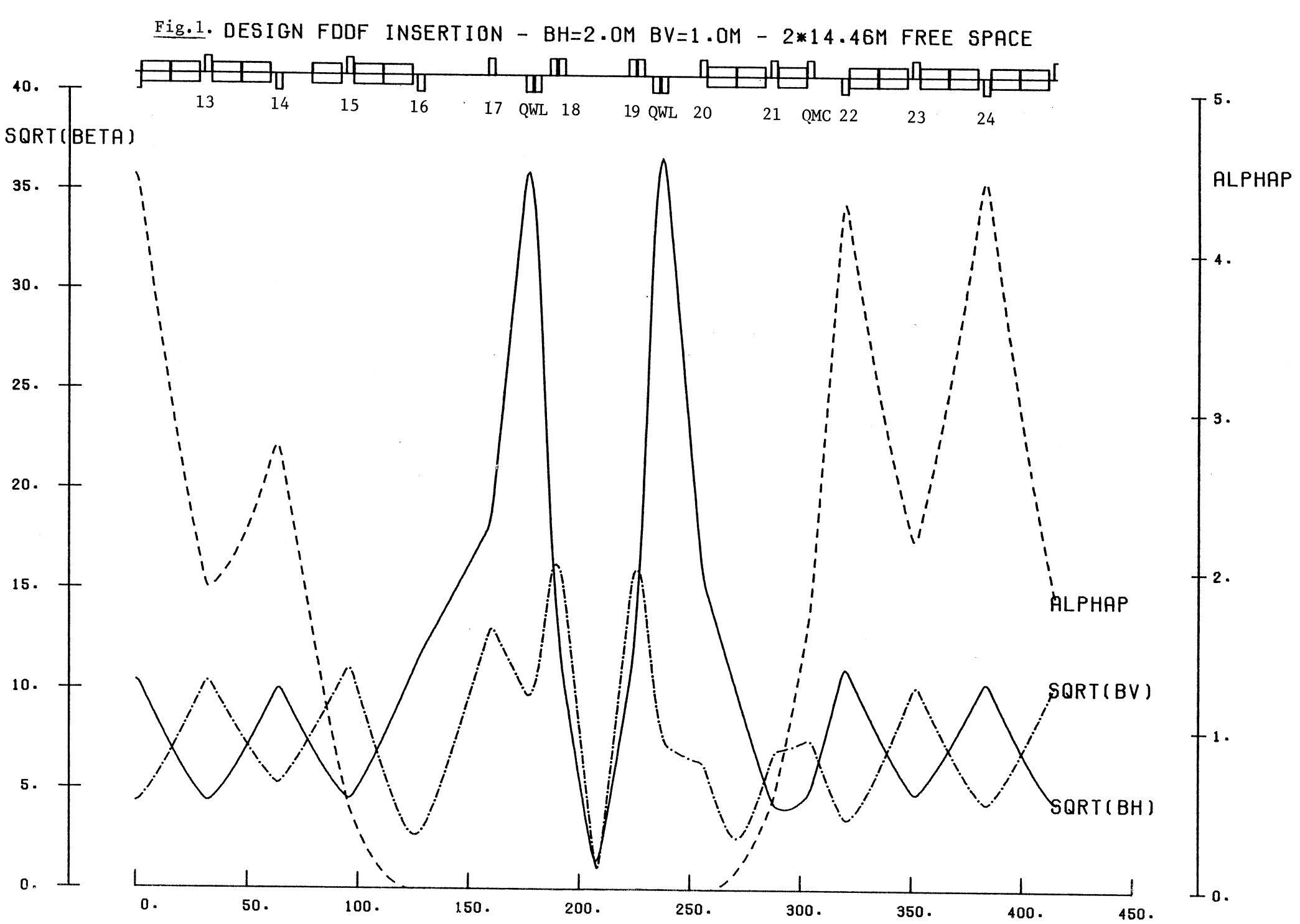
Fig.1. DESIGN FDDF INSERTION - BH=2.0M BV=1.0M - 2*14.46M FREE SPACE
13
14
15
16
17
QWL
18
19
QWL
20
21
QMC
22
23
24
SQRT(BETA)
ALPHAP
40.
35.
30.
25.
20.
15.
10.
5.
0.
5.
4.
3.
2.
1.
0.
0.
50.
100.
150.
200.
250.
300.
350.
400.
450.
ALPHAP
SQRT(BV)
SQRT(BH)

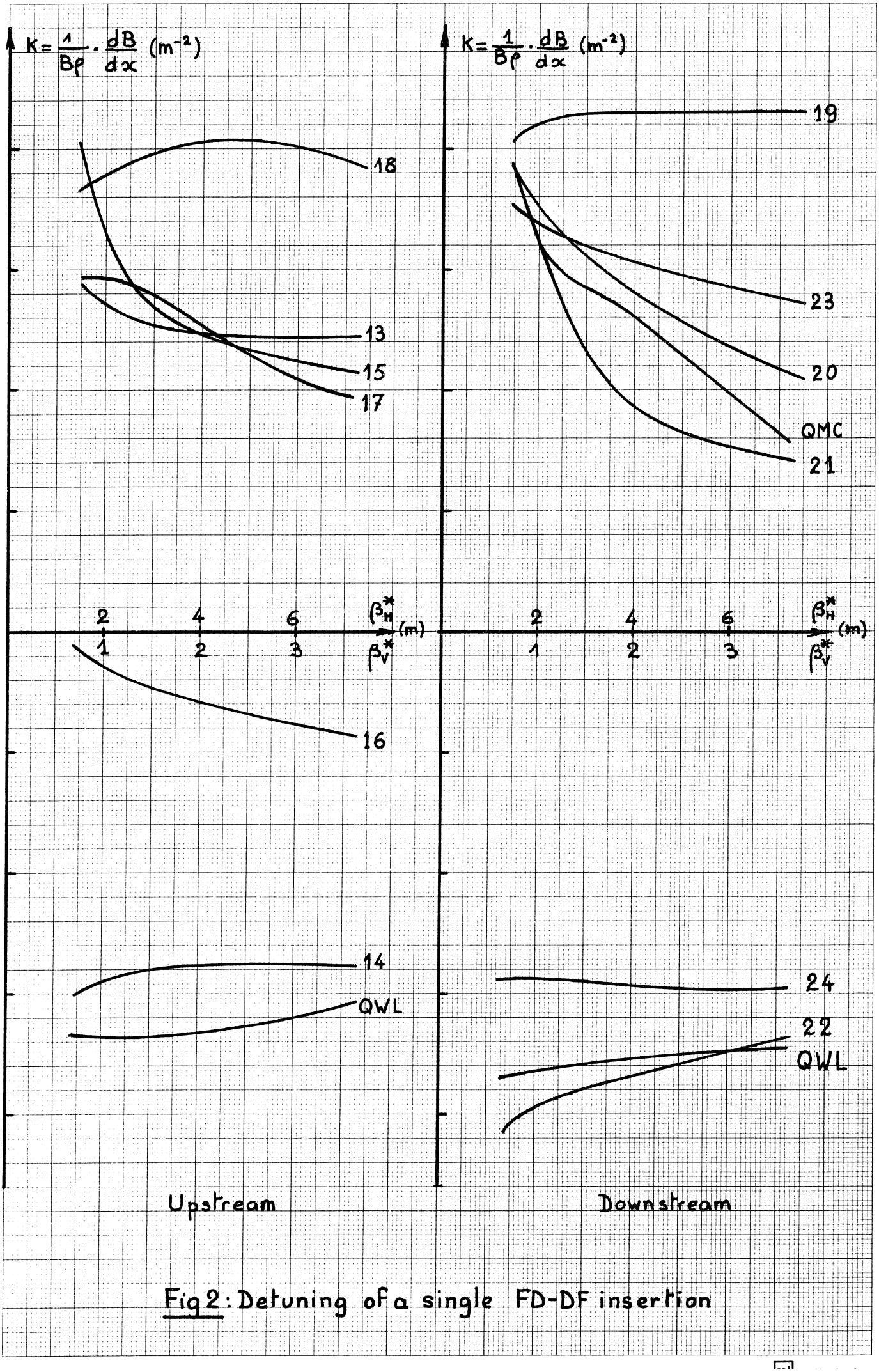


Fig 2 : Detuning of a single FD-DF insertion

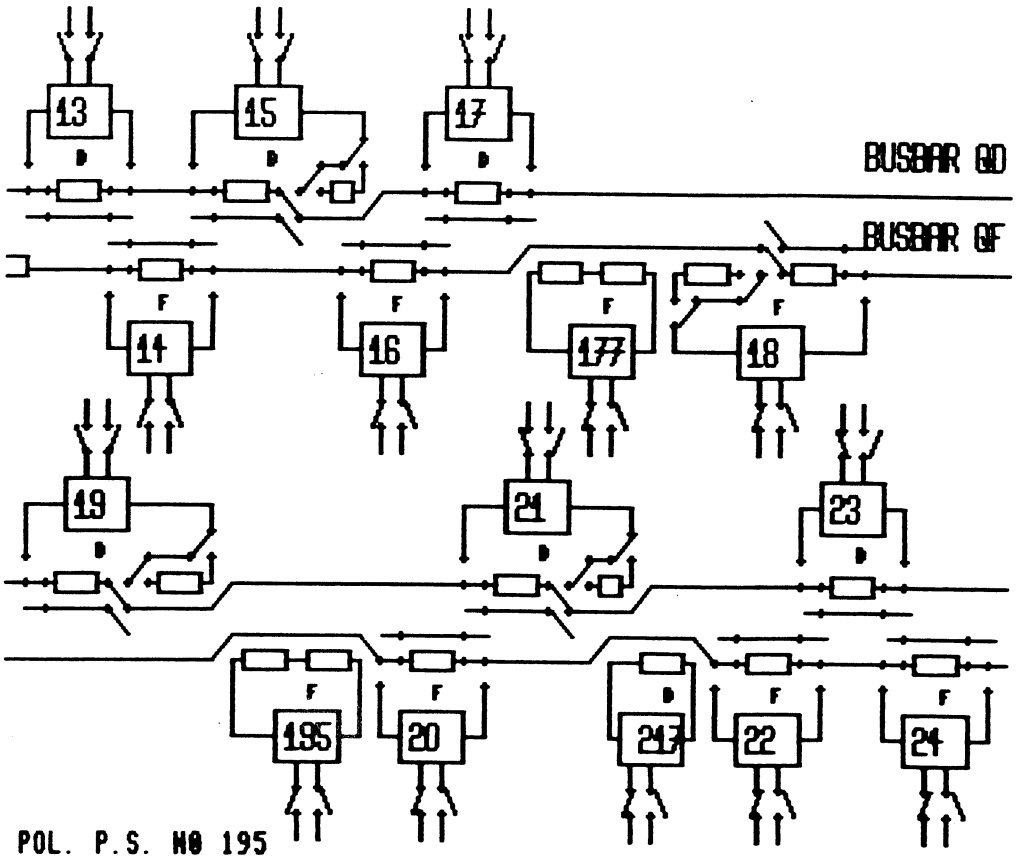


a) LOW BETA OFF

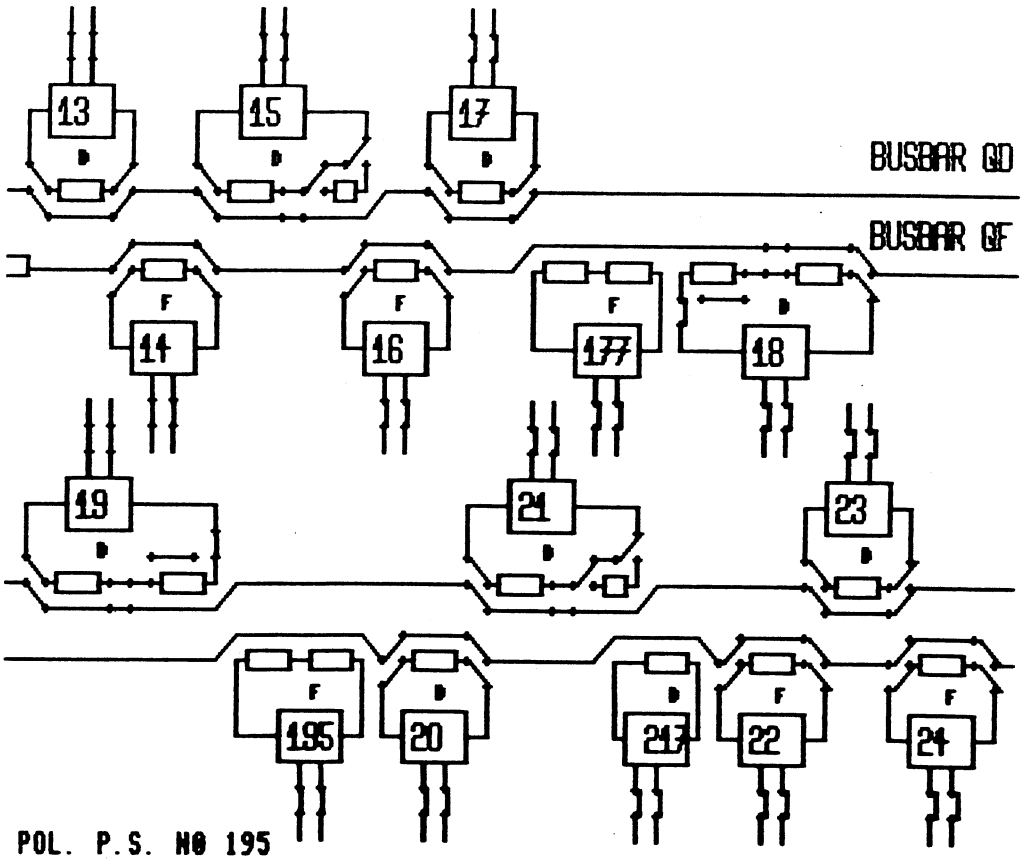


b) LOW BETA ON

Fig3: SWITCHING LOW BETA LSS4 POWER SUPPLIES

| 25 MAR 82 15: 1:52 | ACTIVE CYCLE | NEW CYCLE |
|---|---|---|
| B STATIONS SELECTED | 101110 101110 11 | 101110 101110 11 |
| NO. OF SUBCYCLES | 1 | 1 |
| QH | 26.630 | 26.739 |
| QV | 26.580 | 27.719 |
| INJECTION (GEV/C) | 10.036 | 26.000 |
| DEBUNCHING TIME (S) | 1.260 | 4.860 |
| RAMP TYPE | 1 | 13 |
| NO. OF FLAT TOPS | 2 | 1 |
| FLAT TOP 1 (GEV/C) | 250.0 | |
| FLAT TOP 1 DUR. (S) | 2.040 | |
| FLAT TOP 2 (GEV/C) | 400.0 | 270.0 |
| FLAT TOP 2 DUR. (S) | 2.100 | 2.880 |
| TOTAL CYCLE TIME (S) | 12.000 | 14.400 |
| SQUEEZING FACTOR | 0 | 21.79 |
| LOW BETA P.S. LSS4 | OFF | DFDFD FDDF DDDFDF |
| LOW BETA P.S. LSS5 | OFF | DFDFD FDDF DDDFDF |
| DEAD TIME (S) | .96 | .36 |
| FILENAME | Normal operation | CYCLEI<br>with 2 low-betas |

Fig. 4 Cycle ini[illegible]

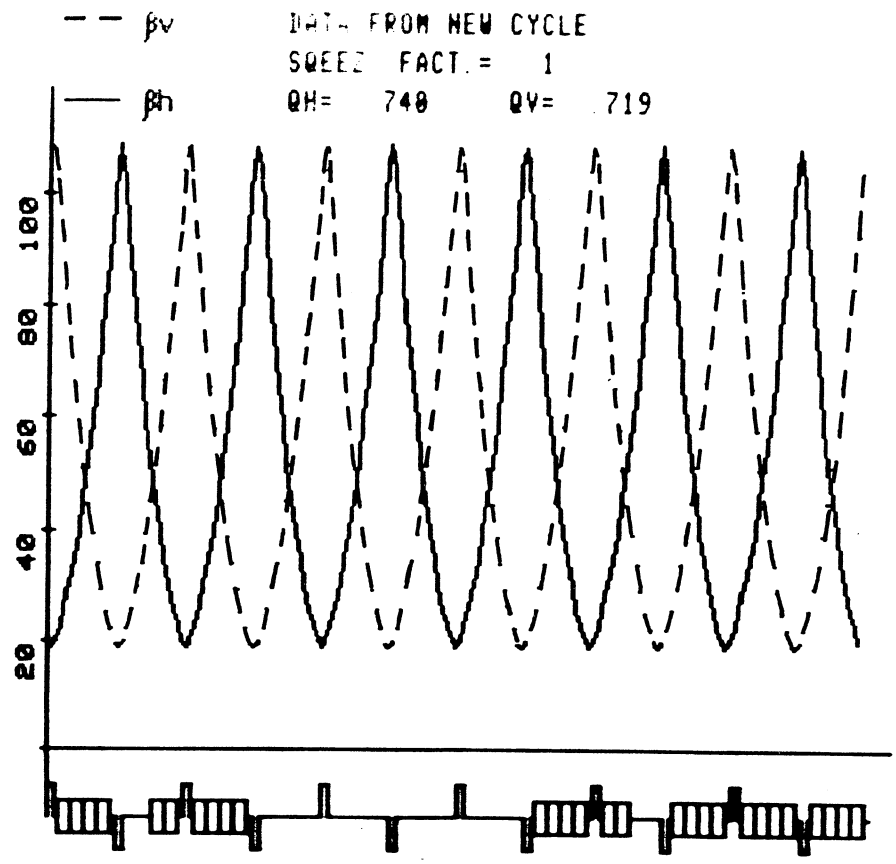


a) matched insertion

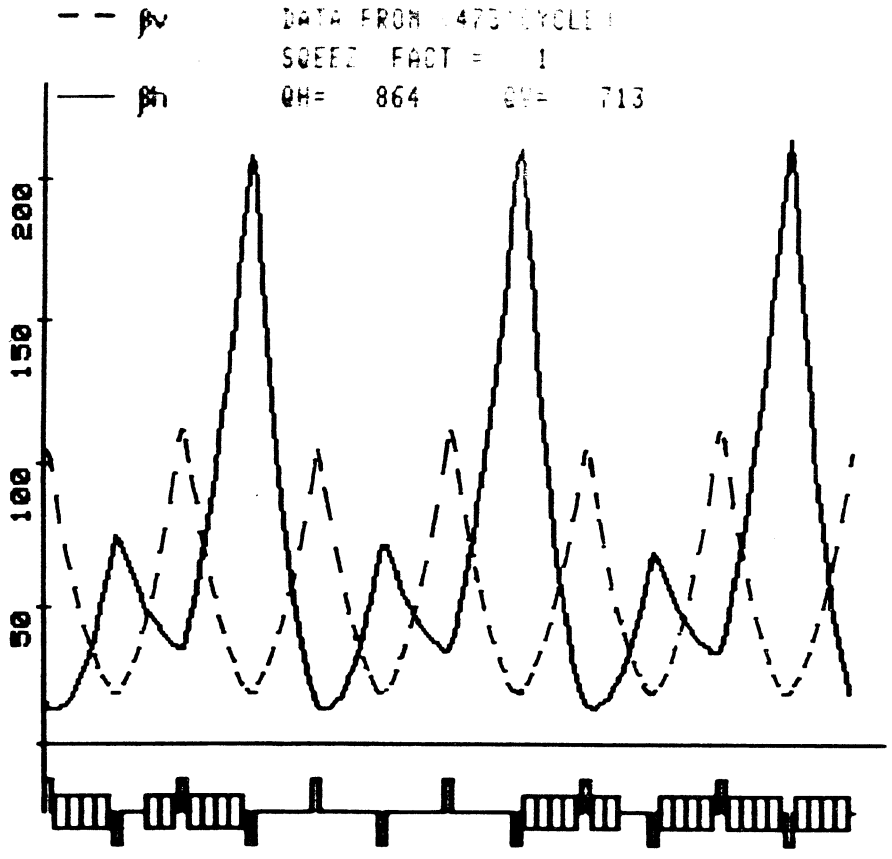


b) error of 2% in QWL pairs

Fig. 5 Betatronic functions in LSS1

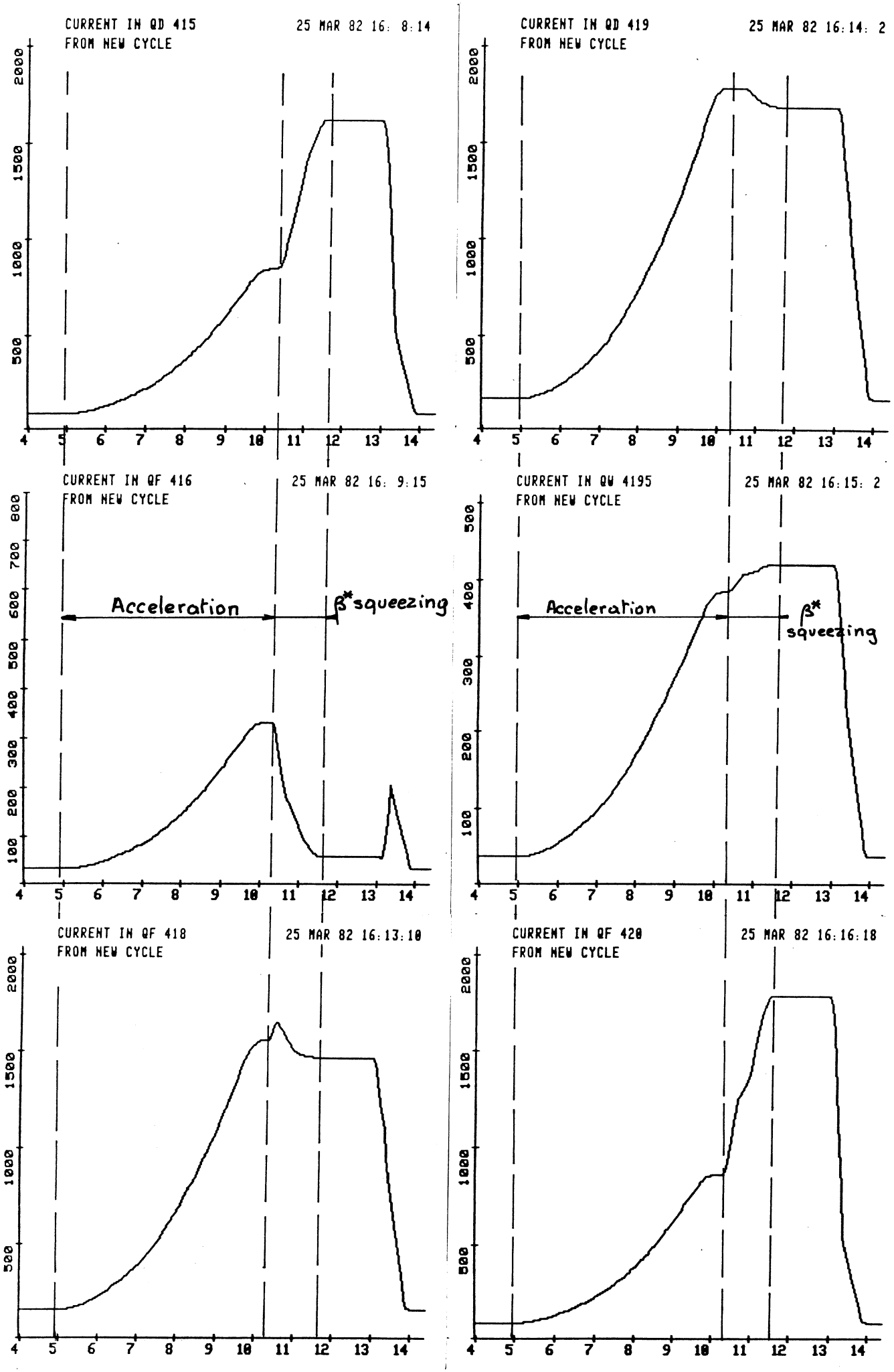


Fig. 6 Some current waveforms for one squeezed insertion

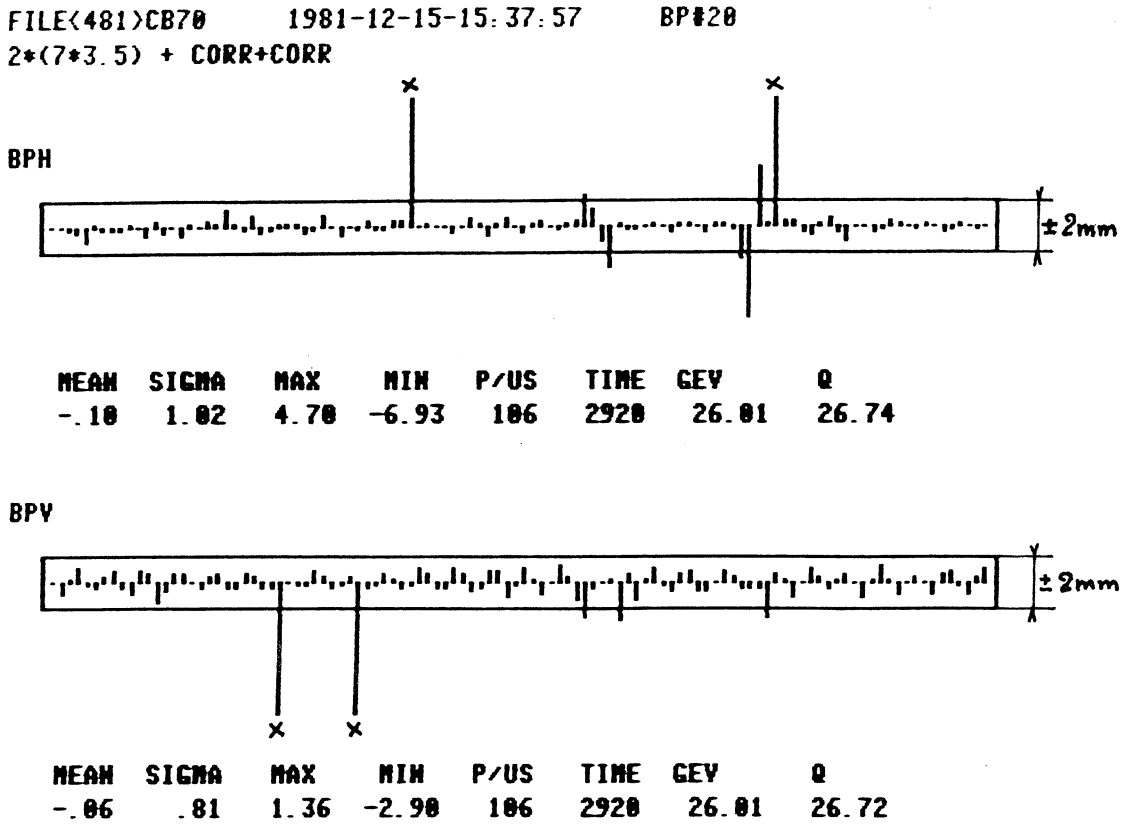


Fig. 7 26 GeV orbit for 2 constant insertions

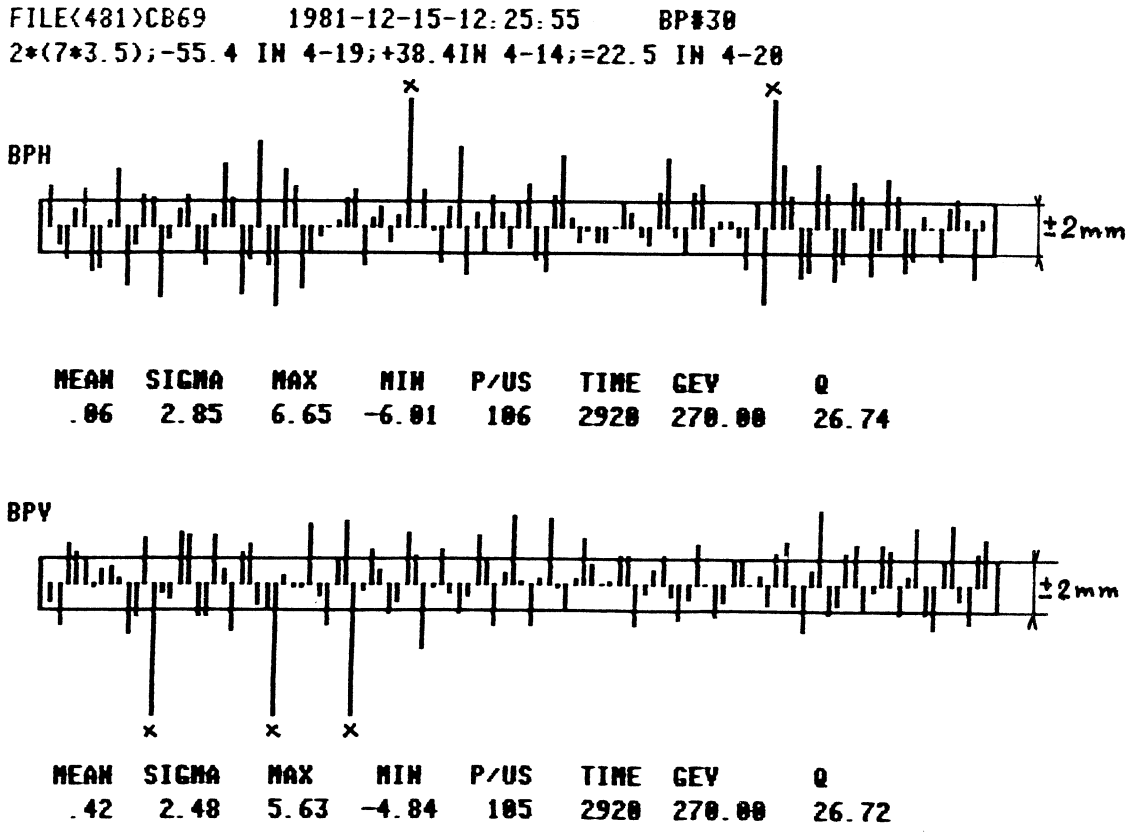


Fig. 8 270 GeV orbit with 2 constant insertions

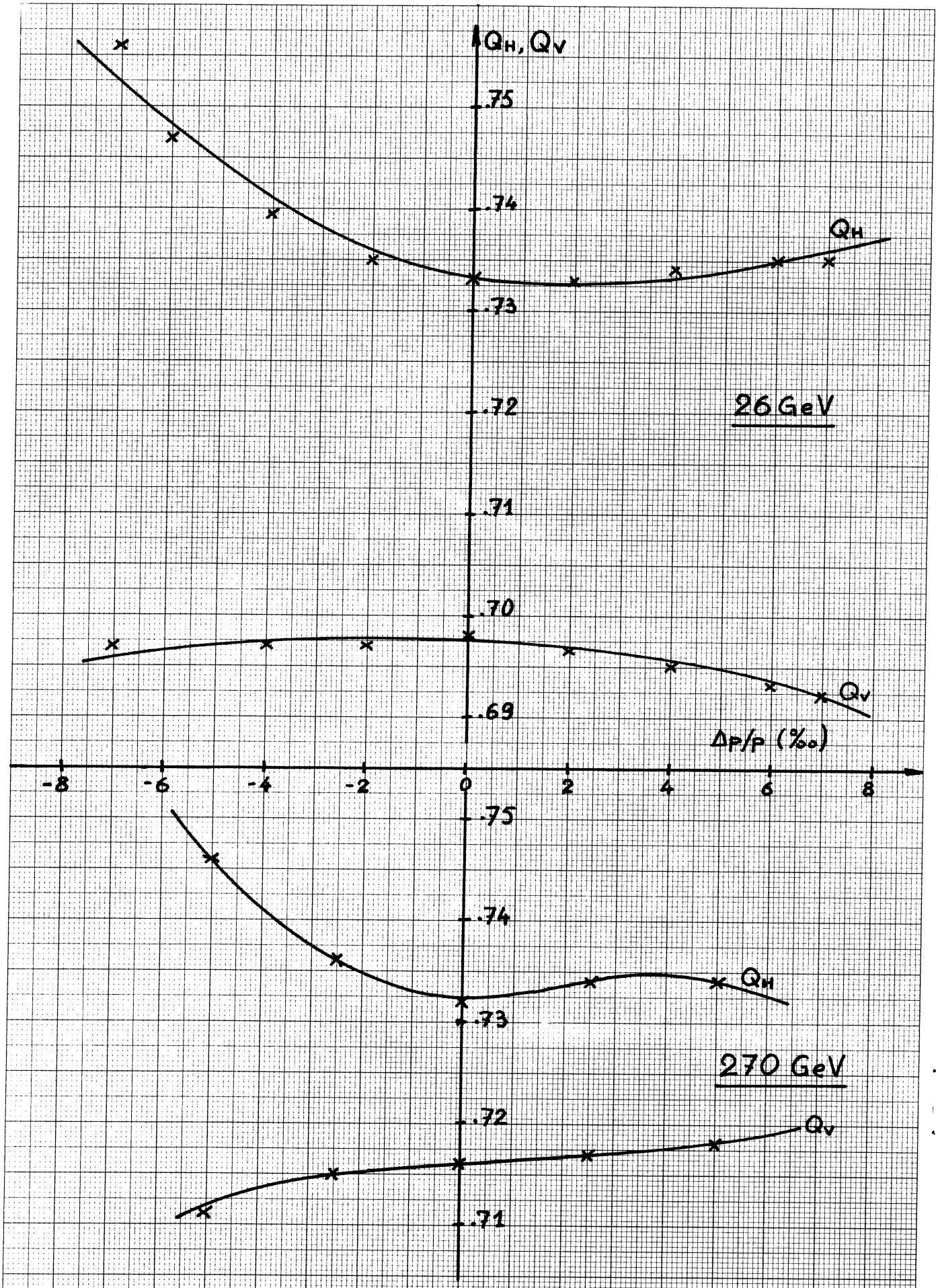


Fig 9: Chromaticities for 2 constant insertions

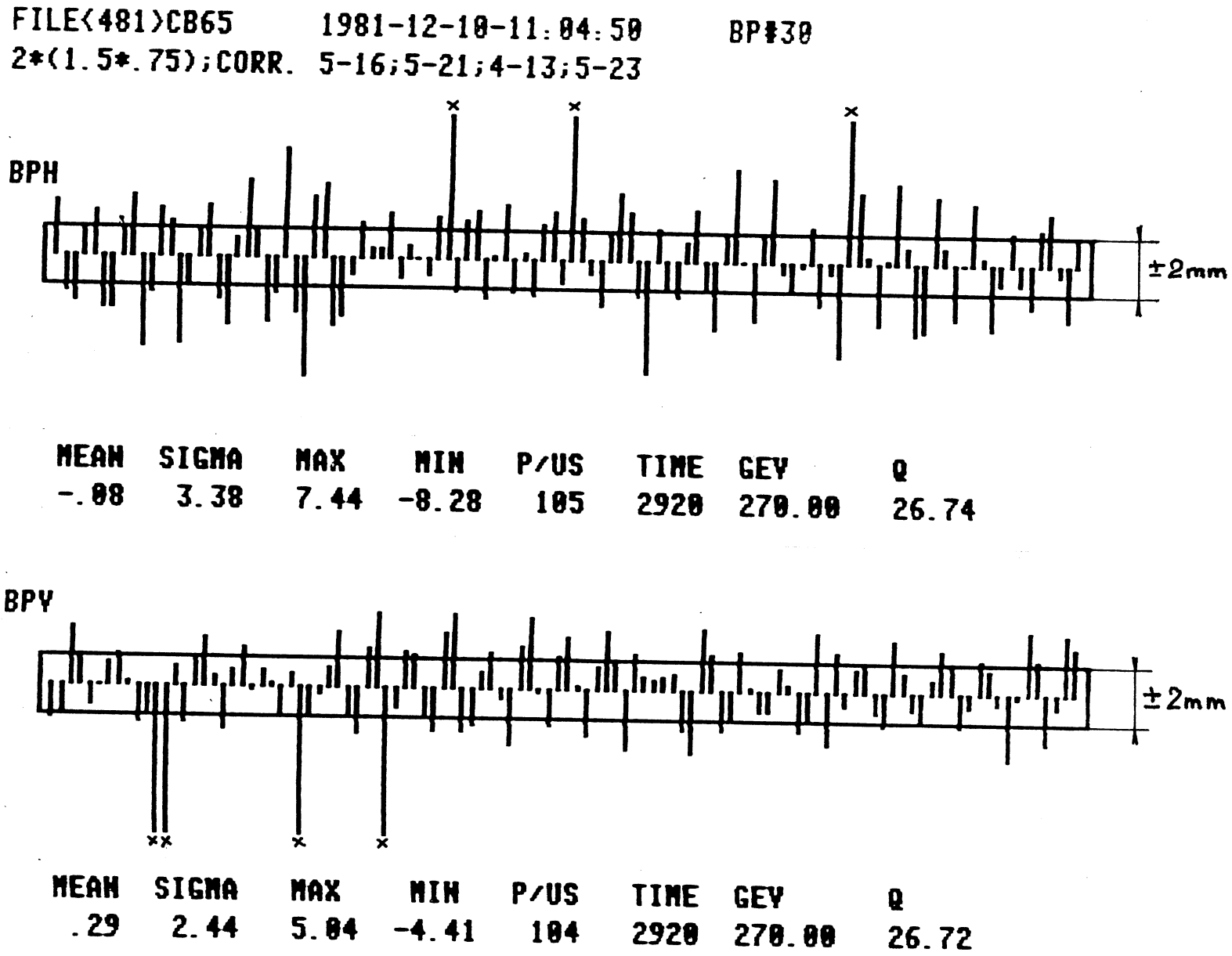


Fig. 10 270 GeV orbit with 2 squeezed insertions

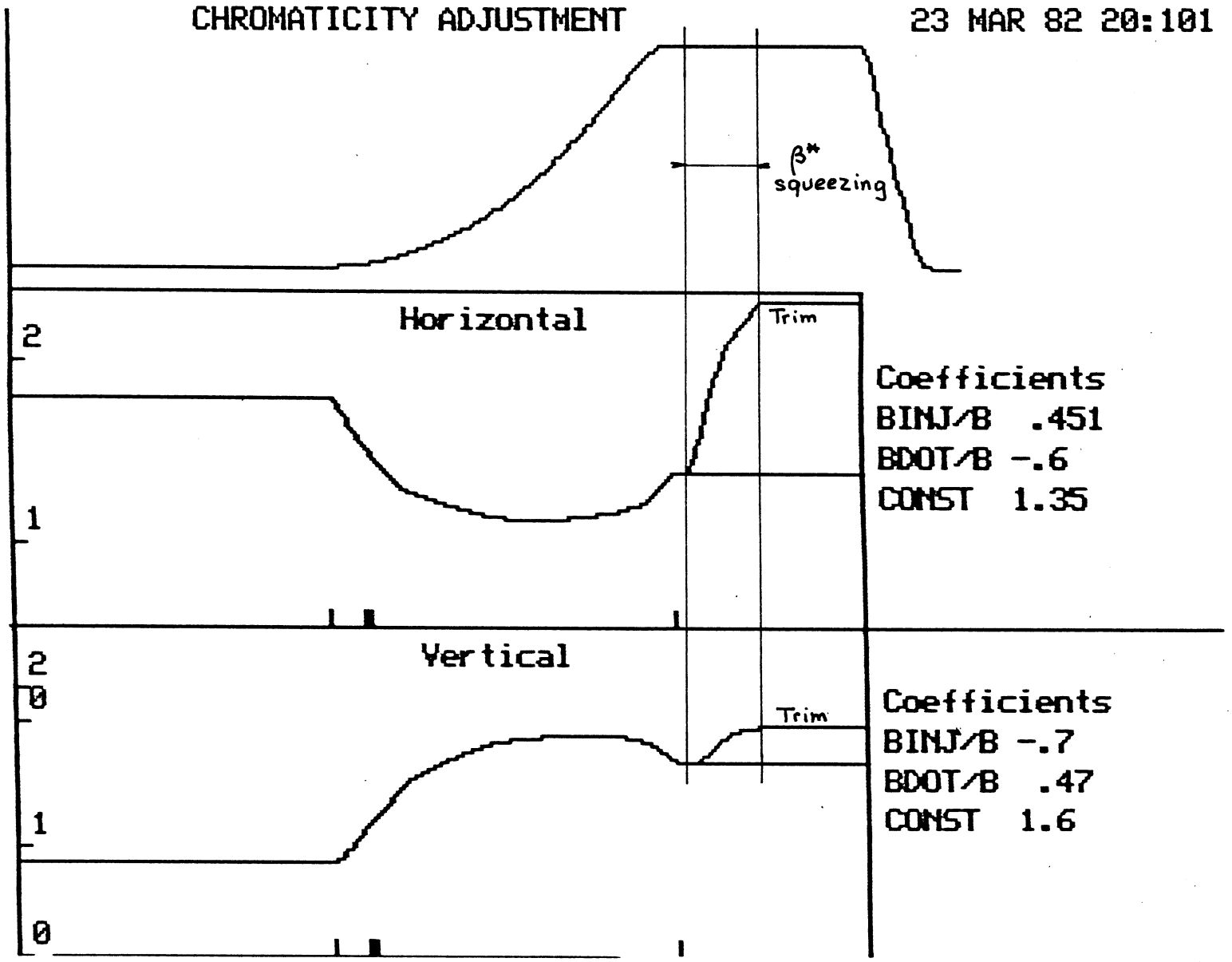


Fig. 11 Chromatic adjustments during squeezing

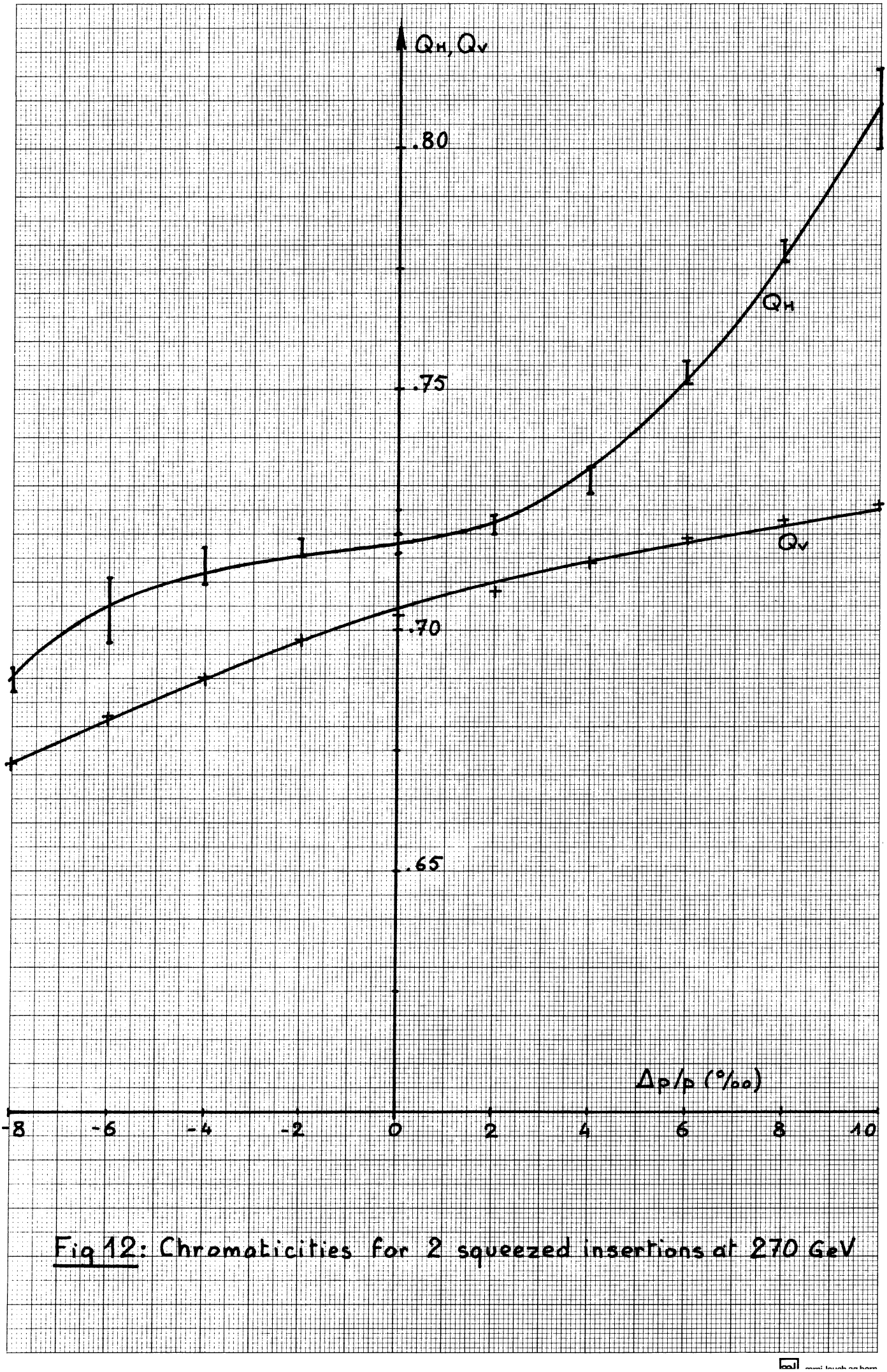


Fig 12: Chromaticities for 2 squeezed insertions at 270 GeV

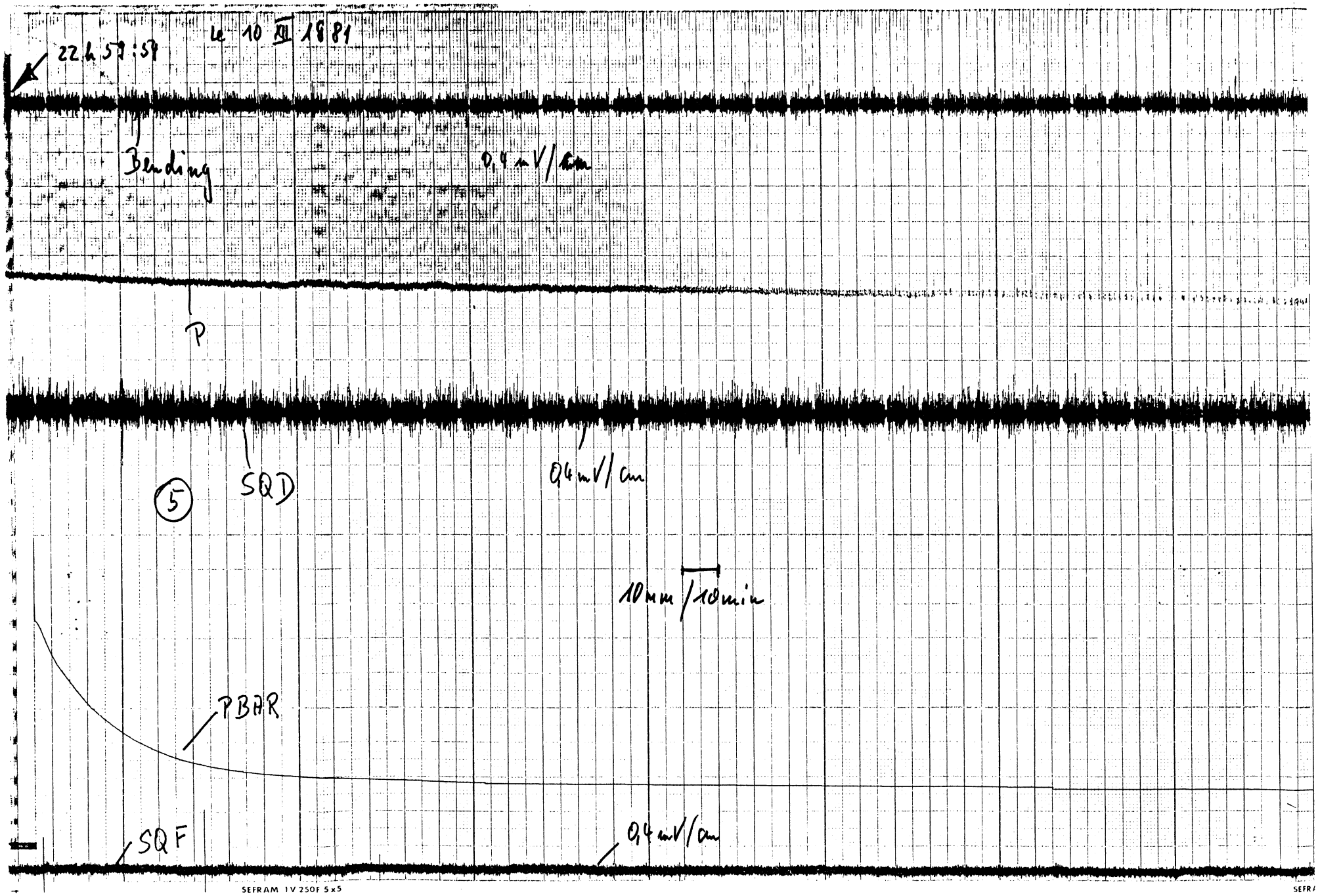


Fig. 13 Beam currents during storage with 2 squeezed insertions